Journal of Cerebral Blood Flow & Metabolism (2011) 31, 1599–1611

www.jcbfm.com

Physiological origin for the BOLD poststimulus undershoot in human brain: vascular compliance versus oxygen metabolism

Jun Hua[1,2], Robert D Stevens[1,2,3], Alan J Huang[1,2,4], James J Pekar[1,2] and Peter CM van Zijl[1,2]

[1]*Russell H Morgan Department of Radiology and Radiological Science, Division of MR Research, Johns Hopkins University School of Medicine, Baltimore, Maryland, USA;* [2]*F.M. Kirby Center for Functional Brain Imaging, Kennedy Krieger Institute, Baltimore, Maryland, USA;* [3]*Department of Anesthesiology Critical Care Medicine and Neurology, Johns Hopkins University School of Medicine, Baltimore, Maryland, USA;* [4]*Department of Biomedical Engineering, Johns Hopkins University School of Medicine, Baltimore, Maryland, USA*

The poststimulus blood oxygenation level-dependent (BOLD) undershoot has been attributed to two main plausible origins: delayed vascular compliance based on delayed cerebral blood volume (CBV) recovery and a sustained increased oxygen metabolism after stimulus cessation. To investigate these contributions, multimodal functional magnetic resonance imaging was employed to monitor responses of BOLD, cerebral blood flow (CBF), total CBV, and arterial CBV (CBV_a) in human visual cortex after brief breath hold and visual stimulation. In visual experiments, after stimulus cessation, CBV_a was restored to baseline in 7.9 ± 3.4 seconds, and CBF and CBV in 14.8 ± 5.0 seconds and 16.1 ± 5.8 seconds, respectively, all significantly faster than BOLD signal recovery after undershoot (28.1 ± 5.5 seconds). During the BOLD undershoot, postarterial CBV (CBV_{pa}, capillaries and venules) was slightly elevated ($2.4 \pm 1.8\%$), and cerebral metabolic rate of oxygen ($CMRO_2$) was above baseline ($10.6 \pm 7.4\%$). Following breath hold, however, CBF, CBV, CBV_a and BOLD signals all returned to baseline in $\sim$20 seconds. No significant BOLD undershoot, and residual CBV_{pa} dilation were observed, and $CMRO_2$ did not substantially differ from baseline. These data suggest that both delayed CBV_{pa} recovery and enduring increased oxidative metabolism impact the BOLD undershoot. Using a biophysical model, their relative contributions were estimated to be $19.7 \pm 15.9\%$ and $78.7 \pm 18.6\%$, respectively.
Journal of Cerebral Blood Flow & Metabolism (2011) **31,** 1599–1611; doi:10.1038/jcbfm.2011.35; published online 6 April 2011

Keywords: BOLD undershoot; cerebral blood flow; cerebral blood volume; hypercapnia; MRI; oxygen metabolism

Introduction

Blood oxygenation level-dependent (BOLD) functional magnetic resonance imaging (fMRI) is now the most commonly deployed non-invasive functional brain-imaging technique. On neuronal activation, elevated BOLD signal, which corresponds to ensemble changes in cerebral blood flow (CBF), cerebral blood volume (CBV), and cerebral metabolic rate of oxygen ($CMRO_2$), is detected. Ever since the first functional BOLD experiments, the so-called BOLD poststimulus undershoot, which refers to the transient signal drop below baseline after stimulus cessation, has been consistently observed (Frahm *et al*, 1992; Kwong *et al*, 1992). Considerable effort has gone into investigating the physiological origins of this undershoot, which have potentially valuable inferences on mechanisms of neurovascular coupling. However, there is still no consensus on this issue today. Two main theories are available. The vascular compliance models, including the Balloon model (Buxton *et al*, 1998) and the Windkessel model (Mandeville *et al*, 1999), postulate that the poststimulus undershoot is mainly because of a temporal mismatch between CBF and CBV changes after stimulus cessation, whereas $CMRO_2$ is still tightly coupled with CBF. Experimental evidence supporting this hypothesis is a delayed return of

Correspondence: Dr J Hua or PCM van Zijl, Russell H Morgan Department of Radiology and Radiological Science, Division of MR Research, Johns Hopkins University School of Medicine, 720 Rutland Avenue, Baltimore, MD 21205, USA.
E-mail: jhua@mri.jhu.edu or pvanzijl@jhu.edu
This publication was made possible by grant support from NIH-NIBIB R01-EB004130 and NIH-NCRR P41-RR15241.
Received 3 November 2010; revised 17 February 2011; accepted 2 March 2011; published online 6 April 2011

CBV (relative to CBF) during BOLD undershoot observed using laser Doppler flowmetry CBF measurement and monocrystalline iron oxide nanoparticle (MION) contrast-enhanced MRI measurement of CBV in rat somatosensory cortex (Mandeville *et al*, 1998). Similar observations were reported in a number of studies, most of which showing CBV changes in animal cortex under anesthesia using steady-state blood-pool contrast-agent-enhanced MRI (Kida *et al*, 2007; Kim *et al*, 2007) or optical-imaging techniques (Jones *et al*, 2001). In addition, the vascular compliance theory was also extended to include potential contribution from a CBF undershoot after stimulus cessation (Chen and Pike, 2009). Conversely, the metabolic hypothesis (Frahm *et al*, 1996; Kruger *et al*, 1996) attributes the BOLD undershoot predominantly to a transient uncoupling of CBF and $CMRO_2$. Lu *et al* (2004*b*), using CBF and CBV responses from arterial spin labeling (ASL) MRI (Golay *et al*, 1999) and vascular space occupancy (VASO) MRI (Lu *et al*, 2003), respectively, found that both CBF and CBV returned to baseline shortly after visual stimulus cessation, right around the time when the BOLD undershoot starts, whereas $CMRO_2$ was shown to remain elevated during the entire undershoot period. Similar results were demonstrated in normal human visual cortex using various CBV-imaging approaches: VASO (Donahue *et al*, 2009; Poser and Norris, 2007; Tuunanen *et al*, 2006), bolus tracking of exogenous paramagnetic contrast agent (Frahm *et al*, 2008), steady-state blood-pool contrast-agent-enhanced MRI (Blockley *et al*, 2009; Dechent *et al*, 2011), as well as optical-imaging approaches (Schroeter *et al*, 2006). In addition to the absence of a delayed CBV recovery, the metabolic hypothesis is also supported by several other studies (Nagaoka *et al*, 2006; Poser *et al*, 2011). For instance, under hypotension in cat visual cortex where no significant CBV dilation is detected, the BOLD response to visual stimulation became negative for a period of $\sim$20 seconds after stimulation termination, indicating continued oxygen metabolism (Nagaoka *et al*, 2006). More recent studies suggest that both mechanisms may contribute, and that their relative contributions may vary spatially. When measuring CBV dynamics in cat brain using MION-enhanced MRI at high field (9.4 T) with a spatial resolution of $0.15 \times 0.15 \times 2\,mm^3$, it was found that CBV in surface vessels returned to baseline quickly after stimulus cessation, whereas CBV recovery in tissue was much slower, with the presence of BOLD undershoot at both locations (Jin and Kim, 2008*a*; Yacoub *et al*, 2006; Zhao *et al*, 2007*a*). These findings imply that the oxygen consumption in tissue (metabolic origin) may be the governing factor in downstream surface vessels, whereas both mechanisms (vascular and metabolic) may have a role in tissue.

In this paper, we employed non-invasive fMRI techniques to monitor the transient responses of BOLD, CBF, arterial and postarterial CBV (CBV_{pa}), and $CMRO_2$ *in vivo* in human visual cortex after brief breath holding and visual stimulation. There are two main difference in this study compared with previous works. First, hypercapnia induced by breath holding or CO_2 inhalation is a global cerebral hemodynamic challenge that is mechanistically distinct from neuronal stimulation. It has been reported that there is no evident BOLD poststimulus undershoot after short-term breath holding (Donahue *et al*, 2009). This provides a unique model to investigate the mechanisms of the BOLD undershoot by monitoring the physiological responses in the absence of the undershoot and comparing them with the ones that are concurrent with it. Second, arterial and postarterial (capillary and venous) blood have different effects on the BOLD signal. Although it is generally accepted that the oxygenation level change in postarterial blood dominates the BOLD effect, it has been suggested (Buxton, 2009) that arterial CBV (CBV_a) alteration also contributes to the BOLD signal owing to the different relaxation rates (R_2 or R^*_2) of fully oxygenated blood and extravascular tissue (Lu and van Zijl, 2005; Zhao *et al*, 2007*b*). Therefore, measuring the CBV changes in arterial and postarterial compartments separately may provide further insights to the origins of BOLD undershoot and clarify some apparent conflicts between the vascular and metabolic hypotheses. Here, by comparing the temporal evolutions of the hemodynamic responses after two different types of stimulation, we sought to clarify the dominant mechanism and estimate the amount to which each mechanism (vascular and metabolic) contribute to the BOLD poststimulus undershoot after neuronal activation.

Materials and methods

Experiment

This study was approved by the Johns Hopkins Institutional Review Board and complied with the Health Insurance Portability and Accountability Act. All measurements were conducted on a 3.0 T (3T) clinical MRI scanner (Philips Medical Systems, Best, the Netherlands) with 11 healthy subjects (five women and six men, age 23 to 52 years) who have given written informed consent before participation. An MR-compatible Invivo patient-monitoring system (Invivo Research Inc., Orlando, FL, USA) was used to record heart rate, arterial oxygen saturation level (S_{aO2}), and end-tidal CO_2 before, during, and after each fMRI task session. Blood pressure and body temperature (Braun, ThermoScan Pro 3000, Kronberg, Germany) were also recorded for each participant on arrival and after completion of all experiments.

A total of eight fMRI sessions were performed for each participant, including BOLD, CBF, CBV, and CBV_a measurements during a visual task and a breath-hold task, respectively. The visual task consisted of four blocks of alternating 55-second cross-hair fixation and 15-second black/white flashing (frequency = 8 Hz) checkerboard stimulation, with an additional 55-second cross-hair fixation at the end of the fourth block. The breath-hold task

consisted of four blocks of 50-second normal breathing, 5-second exhaling, and 15-second breath holding, followed by an additional 55-second normal breathing. The two tasks were interleaved for each subject, with the order of different modalities pseudorandomized. The breath-holding duration was optimized (Donahue *et al*, 2009) to avoid extra respiratory compensation after breath hold, which would affect poststimulus hemodynamics. Participants were instructed to refrain from using hemodynamic stimulants (coffee, tea, chocolate, and licorice) for 6 hours before their participation, and also to arrive at least 15 minutes before the start of study to rehearse the paradigms.

A body coil ($\sim$650 mm in length) was used for radio frequency (RF) pulse transmission and an 8-channel phased-array head coil was used for reception (sensitivity encoding or SENSE acceleration factor of 2.5 was used). A single slice centered on the calcarine fissure was acquired in CBF, CBV and CBV_a scans, and the location was kept identical for each subject. A single-shot turbo spin echo sequence with minimal effective time of echo (TE) (TE = 6 milliseconds, turbo spin echo factor = 22, readout duration $\approx$130 milliseconds, and half scan = 0.525) was employed for CBF, CBV and CBV_a imaging to suppress the fat shift artifact as well as unwanted BOLD contamination when measuring these physiological parameters (Poser and Norris, 2007). The spatial resolution was identical for all scans: field of view = $192 \times 192\,mm^2$ and voxel size = $3 \times 3 \times 3\,mm^3$. The temporal resolutions (determined by the repetition time (TR)) of all scans were multiples of 2.5 seconds (2.5 seconds for BOLD, CBF and CBV_a, 5 seconds for CBV, see below) so that additional parameters such as CBV_{pa} and $CMRO_2$ could be derived.

The transfer-insensitive-labeling technique (TILT) ASL technique (Golay *et al*, 1999) was employed for CBF imaging: TR/TE = 2.5 seconds/6 milliseconds, labeling slab thickness = 80 mm, gap between label and imaging slice = 12.5 mm, alternate acquisition of label, and control images. To sensitize the contrast predominantly to CBF (amount of blood delivered into tissue per unit time) and avoid overestimation, a long postlabeling delay (1.6 seconds) (Donahue *et al*, 2006*b*) and a pair of bipolar gradients (velocity encoding (V_{enc}) = 3 cm/second) (Francis *et al*, 2008) were applied to allow labeled blood water to reach the capillary exchange site and eliminate residual blood signal originated from upstream arterial vessels.

CBV-weighted imaging was achieved using VASO MRI, in which the blood signal in the brain is zeroed using inversion recovery, and residual tissue signal is employed to infer CBV changes (Lu *et al*, 2003). Recent independent experiments from Jin and Kim (2008*b*) in cat brain with high spatial resolution ($0.31 \times 0.31 \times 2\,mm^3$) showed that VASO signal changes are well localized in middle cortical layers where microvessel density and stimulus evoked neural activity are greatest. When long TR (> 3 seconds) is used, the VASO contrast is specifically sensitive to total CBV alteration, whereas contaminations from CBF, fresh inflowing blood, and partial volume effects are minimal (Donahue *et al*, 2006*a*). Therefore TR/TE/TI (inversion time) = 5 seconds/6 milliseconds/1,054 milliseconds was used.

CBV_a dynamics was detected with a recently developed technique called inflow VASO (iVASO; Hua *et al*, 2009, 2011), in which only arterial blood signal is nulled. This is achieved by using a spin preparation scheme similar to those in ASL methods, where the blood water spins from the feeding arteries are selectively inverted. The difference between iVASO and ASL, however, is that: (1) there is no need for a control scan in iVASO; (2) by using a shorter TI, iVASO is predominantly sensitive to the signal changes from arterial blood water spins before arriving at the capillary network (CBV_a changes), whereas ASL contrast is based on the water exchange effect between blood and tissue within the capillary network to measure CBF. The parameters for iVASO were: TR/TE/TI = 2.5 seconds/6 milliseconds/811 milliseconds, gap between inversion and the imaging slice = 10 mm.

BOLD images were acquired using single-shot gradient echo echo-planar-imaging with TR/TE/FA (flip angle) = 2.5 seconds/45 milliseconds/85° (Ernst angle), echo planar imaging factor = 29, and readout train length $\approx$50 milliseconds per slice. To minimize artifactual activations in large blood vessels caused by inflow, a vascular crushing gradient (b = 50 seconds/mm^2) was used and 15 slices were acquired with the central slice precisely aligned with the single-slice location in other scans. Only the central slice in BOLD experiments was processed and compared with other modalities. Fat suppression was applied to eliminate the fat shift artifact typically seen in gradient echo echo-planar-imaging.

General Data Analysis

Images were coregistered using the automated image registration algorithm (Woods *et al*, 1998). To account for the different distortions in gradient echo echo-planar-imaging (BOLD) and turbo spin echo (CBF/CBV/CBV_a) sequences, the BOLD images were coregistered to the others using an algorithm designed for intermodality image registration (Woods *et al*, 1993). This method has been validated in Woods' work (Woods *et al*, 1993) using images from subjects with fiducial markers on the skull. The mean error was measured to be $\sim$1.3 mm, which is sufficiently accurate for the current study with $3 \times 3 \times 3\,mm^3$ voxel size. Temporal baseline drift for each voxel was corrected using a cubic spline interpolation routine. The CBF-weighted difference images in ASL were obtained using a surround subtraction method, in which the label/control image is subtracted by the linear interpolation between the surrounding control/label images (Lu *et al*, 2006). This reduces BOLD contamination in ASL scans to avoid artifactual CBF undershoots and restores the nominal temporal resolution to one TR (it takes two TRs to acquire a pair of label and control ASL images). A two-tailed Z-test with statistical significance of 0.01 was engaged to detect activated voxels. Requirements for activation were Z-score ≤ -2.5 (VASO, iVASO), Z-score ≥ 2.5 (BOLD, TILT), and cluster size ≥ 4. Images acquired during 20 seconds at the beginning of the first baseline period and 10 seconds at the beginning of following

baseline and stimulation periods were not included in activation detection.

Only voxels that were activated in all eight scans were subsequently analyzed. Thus, although activated voxels were detected in all regions of gray matter (GM) for breath hold, only occipital area coinciding with voxels activated during visual stimulation were used. The overlapping of the eight activation maps permits a direct comparison with identical voxels activated in both tasks. Besides, the selection of voxels that are activated in all four modalities may help to mitigate artifactual activations in large blood vessels and furnish a more accurate localization of neuronal activity in parenchyma. One data set was excluded from further analysis because of insufficient number of remaining commonly activated voxels, possibly because of severe subject motion during the scans and/or poor task performance. The time course of each parameter was calculated by averaging normalized signals over the commonly activated voxels for each subject. The group averages ($n = 10$) of the time courses are shown in figures and results. Two methods were used to estimate the return time in each time course: (I) the time of first point below baseline after stimulus cessation in each of the four functional blocks was averaged over all blocks and subjects (a total of 40 data points for each return time); (II) in each functional block, the data points between 0 and 25 seconds (approximately the duration of BOLD undershoot) after stimulus cessation were fitted to a cubic spline polynomial. The intersection between the fitted polynomial curve and baseline was taken as the return time, which was then averaged over four blocks and all subjects. Method II is expected to be more robust against large fluctuations in the data. In both methods, baseline was defined as the mean signal intensity of all images acquired more than 5 seconds before and/or 30 seconds after any stimulus period (all signals are expected to be at baseline) plus the noise level, which was estimated with the standard deviation of signal intensities during the same period in each time course. All average changes in BOLD/CBV/CBV_a/CBV_{pa}/$CMRO_2$ during the BOLD undershoot were obtained from time points between 22.5 and 40 seconds after stimulus onset, during which the measured BOLD signal was significantly below baseline. A Student's *t*-test was used to determine significance for comparison between parameters. All data analysis programs (except for automated image registration) were coded in Matlab 6.0 (Mathworks, Natick, MA, USA).

Quantification of Changes in Physiological Parameters

All signal changes are presented as a percentage of baseline value. Note that because our CBV measurements have the lowest temporal resolution (5 seconds), any parameter derived from $\Delta CBV/CBV^{base}$, including $\Delta CBV_{pa}/CBV_{pa}^{base}$ and $\Delta CMRO_2/CMRO_2^{base}$, will have the same temporal resolution. Quantities were computed first for each subject before averaging over the group. The reported standard deviations represent intersubject variation.

For long TR VASO MRI, the relative signal change $\Delta S_{VASO}/S_{VASO}^{base}$ is dominated by ΔCBV in parenchyma (Donahue *et al*, 2006*a*), which can be quantified by (Donahue *et al*, 2006*a*; Lu *et al*, 2003):

$$\frac{\Delta CBV}{CBV^{base}} = \frac{CBV^{act} - CBV^{base}}{CBV^{base}} = \left(\frac{C_{par} - CBV^{base} \cdot C_{blood}}{CBV^{base} \cdot C_{blood}}\right) \cdot \left(-\frac{\Delta S_{VASO}}{S_{VASO}^{base}}\right) \quad (1)$$

where $C_{par} = 0.89$ and $C_{blood} = 0.87$ are the water contents in mL water/mL substance for parenchyma and blood, respectively. A baseline parenchymal blood volume for human brain GM (CBV^{base}) of 0.055 mL blood/mL parenchyma was assumed (Lu *et al*, 2005). CBV^{act} represents CBV during activation.

The CBF and CBV_a changes can be estimated from TILT ASL and iVASO signal changes, respectively. In principle, the contrasts in both methods are also affected by the arterial transit time changes during activation. For TILT ASL, when long TI (> 1.6 seconds) is used (Donahue *et al*, 2006*b*), the transit time effects are negligible, and the TILT signal change is directly proportional to CBF change (i.e., $\Delta S_{TILT}/S_{TILT}^{base} = \Delta CBF/CBF^{base}$; Golay *et al*, 1999). For iVASO, as shown in a previous work (Hua *et al*, 2009, 2011), depending on the arterial transit times in different regions of the cerebral cortex, optimal TR ranges can be derived where the iVASO signal change is dominated by CBV_a alteration alone. For GM in human visual cortex (Francis *et al*, 2008), this optimal TR range was found to be 1.5 to 2.5 seconds (Hua *et al*, 2009, 2011), within which $\Delta CBV_a/CBV_a^{base}$ can be estimated by (Hua *et al*, 2009, 2011):

$$\frac{\Delta CBV_a}{CBV_a^{base}} = \frac{CBV_a^{act} - CBV_a^{base}}{CBV_a^{base}} = \frac{(C_{par} - CBV^{base} \cdot C_{blood}) \cdot (1 - e^{-TR/T_{1,GM}})}{CBV_a^{base} \cdot C_{blood} \cdot (1 - e^{-TR/T_{1,blood}})} \cdot \left(-\frac{\Delta S_{iVASO}}{S_{iVASO}^{base}}\right) \quad (2)$$

where CBV_a^{base} is assumed to be 0.21 CBV^{base} (van Zijl *et al*, 1998), and $T_1 = 1{,}624$ milliseconds for blood, 1,209 milliseconds for GM tissue at 3T (Lu *et al*, 2004*a*). CBV_{pa} change ($\Delta CBV_{pa}/CBV_{pa}^{base}$) can then be calculated from $\Delta CBV/CBV^{base}$ and $\Delta CBV_a/CBV_a^{base}$.

To estimate $\Delta CMRO_2/CMRO_2^{base}$ during breath-hold and visual tasks from the BOLD, CBF, and CBV measurements, two quantitative BOLD models were used: the model from Lu *et al* (2004*b*) and the Davis model (Davis *et al*, 1998). In the Lu model, the BOLD signal is the sum of three compartments: arterial blood (*a*), postarterial blood (pa), and extravascular tissue (*t*):

$$S_{BOLD}^i \sim CBV_a^i \cdot M_a \cdot e^{-R_{2a}^{*,i} \cdot TE} + CBV_{pa}^i \cdot M_{pa} \cdot e^{-R_{2pa}^{*,i} \cdot TE} + (C_{par} - CBV^i \cdot C_{blood}) \cdot M_t \cdot e^{-R_{2t}^{*,i} \cdot TE},\ i = \text{base, act} \quad (3)$$

where M_j denotes the magnetization in each compartment:

$$M_j = \frac{1 - e^{-R_{1j} \cdot TR}}{1 - \cos(FA) \cdot e^{-R_{1j} \cdot TR}} \cdot \sin(FA),\ j = a, pa, t \quad (4)$$

which depends on acquisition parameters (TR, FA) and longitudinal relaxation rates $R_{1j} = 1/T_{1j}$. Note that the

original Lu model assumed $CBV_a = 0.3$ CBV, and that the fraction does not change during activation. Although this assumption does not substantially undermine the $CMRO_2$ calculation, it could result in 2% to 5% overestimation or underestimation of $CMRO_2$ changes (Lin *et al*, 2008). Therefore, in this study, the CBV_a dynamics measured by iVASO MRI are incorporated into equation (3). The effective transverse relaxation rate (R^*_{2k}) for blood is strongly dependent on its oxygenation fraction Y_k ($Y_k = 0.98$ for arterial blood at both baseline and activation, 0.61 for venous blood at baseline), which can be determined with (Zhao *et al*, 2007*b*):

$$R^*_{2k} = 20.7 + 181(1 - Y_k)^2,\ k = a,\ \text{pa} \tag{5}$$

$R^{*\text{base}}_{2t}$ (R^*_2 of extravascular tissue, excluding all blood compartments) at 3T was measured in Lu and van Zijl (2005) to be 21.15/second and ΔR^*_{2t} during activation can be calculated from (Lu *et al*, 2004*b*):

$$\Delta R^*_{2t} = \gamma \cdot B_0 \cdot \frac{4}{3}\pi \cdot \Delta\chi \cdot Hct \cdot (\text{CBV}^{\text{act}}_{\text{pa}} \cdot (1 - Y^{\text{act}}_v) - \text{CBV}^{\text{base}}_{\text{pa}} \cdot (1 - Y^{\text{base}}_v)) \tag{6}$$

in which $\gamma = 42.58$ MHz/T is the gyromagnetic ratio for hydrogen, $B_0 = 3$T is the strength of main magnetic field, $\Delta\chi = 0.31$ p.p.m. is the susceptibility difference between fully oxygenated and deoxygenated blood, $Hct = 0.36$ is the hematocrit fraction of blood in microvasculature. Using equation (3), the measured BOLD signal change can be modeled as:

$$\frac{\Delta S_{\text{BOLD}}}{S^{\text{base}}_{\text{BOLD}}} = \frac{S^{\text{act}}_{\text{BOLD}} - S^{\text{base}}_{\text{BOLD}}}{S^{\text{base}}_{\text{BOLD}}} \tag{7}$$

and the only remaining unknown parameter, Y^{act}_v, can be solved numerically and used to calculate the $CMRO_2$ change. The relationship between Y_v, Y_a, CBF, and $CMRO_2$ is characterized by (van Zijl *et al*, 1998):

$$1 - Y_v = 1 - Y_a + \text{OEF} \cdot Y_a \tag{8}$$

$$\text{CMRO}_2 = \text{OEF} \cdot \text{CBF} \cdot C_a \tag{9}$$

in which OEF is the oxygen extraction fraction. When the arterial oxygen content (C_a) is constant, the relative $CMRO_2$ change is determined by:

$$\frac{\Delta\text{CMRO}_2}{\text{CMRO}^{\text{base}}_2} = \left(1 + \frac{\Delta\text{OEF}}{\text{OEF}^{\text{base}}}\right) \cdot \left(1 + \frac{\Delta\text{CBF}}{\text{CBF}^{\text{base}}}\right) - 1 \tag{10}$$

The Davis model (Davis *et al*, 1998) requires a calibration factor M that can be calculated from BOLD and CBF signal changes during hypercapnia. Lin *et al* (2008) have demonstrated that using dynamic $\Delta\text{CBV}/\text{CBV}^{\text{base}}$ measurements from breath-hold and visual tasks to compute M and $\Delta\text{CMRO}_2/\text{CMRO}^{\text{base}}_2$, respectively, improves the accuracy compared with estimating the blood volume change from measured $\Delta\text{CBF}/\text{CBF}^{\text{base}}$ with Grubb's empirical equation. Thus M can be calculated from BOLD, CBF, and CBV measurements during breath hold:

$$M = \frac{\Delta\text{BOLD}}{\text{BOLD}^{\text{base}}} \Big/ \left(1 - \left(1 + \frac{\Delta\text{CBV}}{\text{CBV}^{\text{base}}}\right) \cdot \left(1 + \frac{\Delta\text{CBF}}{\text{CBF}^{\text{base}}}\right)^{-\beta}\right) \tag{11}$$

in which $\beta = 1.5$ is a constant determined in Davis *et al* (1998). Relative $CMRO_2$ change can be calculated with:

$$\frac{\Delta\text{CMRO}_2}{\text{CMRO}^{\text{base}}_2} = \left(1 - \frac{1}{M} \cdot \frac{\Delta\text{BOLD}}{\text{BOLD}^{\text{base}}}\right)^{1/\beta} \cdot \left(1 + \frac{\Delta\text{CBV}}{\text{CBV}^{\text{base}}}\right)^{-1/\beta} \cdot \left(1 + \frac{\Delta\text{CBF}}{\text{CBF}^{\text{base}}}\right) - 1 \tag{12}$$

Notice that the Davis model does not take into account CBV_a dynamics separately from CBV, and can only estimate $\Delta\text{CMRO}_2/\text{CMRO}^{\text{base}}_2$ during visual stimulation because the BOLD, CBV, and CBF measurements during breath hold are needed for the estimation of M.

Results

The physiological recordings are summarized in Table 1. No significant differences were found in heart rate, S_{aO2} and end-tidal CO_2 between breath-hold and visual experiments, within visual sessions, or between before and after breath-hold tasks ($P > 0.1$). The equivalent end-tidal CO_2 values before and after breath-hold periods ensures that there was no compensatory hyperventilation after breath hold. During the 15-second breath-hold period, the end-tidal CO_2 recordings were 0 in all subjects, confirming that the breath-hold task was performed. No substantial variation ($P > 0.1$) was found in body temperature (before: $36.8 \pm 0.5^\circ$C and after: $36.9 \pm 0.6^\circ$C) or blood pressure (before: systolic = 119.5 ± 16.1 mm Hg and diastolic = 63.0 ± 8.3 mm Hg; after: systolic = 118.5 ± 9.4 mm Hg and diastolic = 37.0 ± 7.7 mm Hg) between the beginning of first experiment and conclusion of all eight functional sessions.

In this paper, we focus on the hemodynamic changes after stimulus cessation. For that reason, although the signal changes during stimulation are also shown, they are not discussed. The average time courses of relative changes ($\Delta S/S^{\text{base}}$) in CBF, CBV, CBV_a, and BOLD signals over all blocks ($n = 4$) in each session and all subjects ($n = 10$) are displayed in Figures 1A and 1B for breath-hold and Figures 1C and 1D for visual tasks. The BOLD undershoot is evident after visual stimulation and of approximately the same length as the stimulation period, with a peak amplitude of approximately 50% of the peak positive BOLD signal change. No undershoot was found after brief breath hold, consistent with previous reports (Donahue *et al*, 2009). The average time for each time course to reach baseline after the stimulus offset is summarized in Table 2. The return times estimated by methods I and II were not statistically different ($P > 0.1$). It can be seen (Figure 1 and Table 2) that, after breath hold, all four time courses returned to baseline at approximately the same time (all ~ 20 seconds after breath-hold ends, $P > 0.1$). After visual stimulation, the CBV_a

Table 1 Physiological recordings before, during, and after breath-hold and visual tasks

	Breath hold			*Visual*		
	HR[a]	S_{aO2}[b]	$EtCO_2$[c]	*HR*	S_{aO2}	$EtCO_2$
CBF (TILT)						
Before	68.6 ± 8.3	96.8 ± 0.3	44.5 ± 2.5	68.9 ± 6.6	97.1 ± 0.3	44.1 ± 1.9
During	68.8 ± 8.3	97.1 ± 0.6	0.0	67.3 ± 5.9	97.0 ± 0.2	44.4 ± 1.6
After	68.3 ± 7.4	96.8 ± 0.7	44.3 ± 1.7	67.6 ± 6.5	97.3 ± 0.2	43.9 ± 1.9
CBV (VASO)						
Before	69.2 ± 6.6	96.5 ± 0.6	43.8 ± 2.5	67.6 ± 5.3	97.1 ± 0.2	44.2 ± 1.6
During	69.3 ± 7.5	97.3 ± 0.1	0.0	67.6 ± 6.2	97.1 ± 0.2	44.8 ± 1.8
After	68.9 ± 5.8	96.8 ± 0.8	44.1 ± 2.3	67.8 ± 5.8	97.1 ± 0.2	44.8 ± 1.5
CBV_a (iVASO)						
Before	68.4 ± 6.8	96.3 ± 0.5	43.9 ± 2.3	67.9 ± 6.5	96.9 ± 0.2	43.7 ± 1.6
During	67.0 ± 6.6	96.5 ± 0.4	0.0	67.8 ± 6.2	97.3 ± 0.4	44.5 ± 1.6
After	68.9 ± 6.7	96.8 ± 0.8	43.9 ± 2.4	67.4 ± 6.4	97.0 ± 0.4	44.9 ± 1.5
BOLD						
Before	68.6 ± 5.9	96.5 ± 0.2	43.7 ± 1.9	69.2 ± 7.0	96.9 ± 0.4	43.8 ± 1.6
During	68.7 ± 5.7	97.5 ± 0.3	0.0	67.5 ± 6.4	96.9 ± 0.5	43.6 ± 1.3
After	68.5 ± 6.1	96.1 ± 0.7	44.0 ± 2.0	67.2 ± 6.5	97.3 ± 0.5	44.8 ± 1.4

BOLD, blood oxygenation level dependent; CBF, cerebral blood flow; CBV, cerebral blood volume; CBV_a, arterial CBV; $EtCO_2$, end-tidal CO_2; HR, heart rate; iVASO, inflow vascular space occupancy; S_{aO2}, arterial oxygen saturation level; TILT, transfer-insensitive-labeling technique.

[a]HR in beats/minute.

[b]S_{aO2} ($= 100 \times Y_a$) in percentile.

[c]$EtCO_2$ in mm Hg.

Average and standard deviation values (mean ± s.d.) over all subjects ($n = 10$) and task blocks ($n = 4$) are displayed.

time course returned to baseline significantly faster than the CBF and CBV ($P < 0.01$) time courses, between which no significant time difference was found ($P > 0.1$). The CBF and total CBV time courses after visual stimulation returned to baseline slightly faster than the ones after breath hold ($P < 0.05$). In the visual task, CBF, CBV, and CBV_a were not significantly different from baseline during most of the BOLD undershoot period, in line with previous studies (Blockley *et al*, 2009; Donahue *et al*, 2009; Frahm *et al*, 2008; Lu *et al*, 2004*b*; Poser and Norris, 2007; Tuunanen *et al*, 2006).

The relative changes in CBV, CBV_a, and CBV_{pa} were calculated for each subject, and the average time courses ($n = 10$) for breath-hold and visual sessions are shown in Figures 2A and 2B, respectively. The vasodilation and vasoconstriction in arterial and postarterial compartments occurred approximately simultaneously during breath hold, whereas during visual experiments, CBV_a returned to baseline faster than CBV_{pa}. After visual stimulation, $\Delta CBV/CBV^{base}$ was not significantly elevated from baseline during BOLD undershoot ($P > 0.1$), in line with several previous studies (Blockley *et al*, 2009; Donahue *et al*, 2009; Frahm *et al*, 2008; Lu *et al*, 2004*b*; Poser and Norris, 2007; Tuunanen *et al*, 2006). However, after decomposing $\Delta CBV/CBV^{base}$ into arterial and postarterial components, $\Delta CBV_{pa}/CBV_{pa}^{base}$ during BOLD undershoot (Figure 2B inset) was slightly elevated ($2.4 \pm 1.8\%$, $P < 0.05$), whereas $\Delta CBV_a/CBV_a^{base}$ was not significantly different from baseline ($P > 0.1$). This indicates that during the BOLD undershoot, CBV_a has returned to baseline and the only vasodilation resided in the postarterial compartment ($\Delta CBV = \Delta CBV_{pa}$). When normalizing this small residual change with baseline CBV_{pa} ($\Delta CBV_{pa}/CBV_{pa}^{base}$) rather than the greater baseline total CBV ($\Delta CBV/CBV^{base} = \Delta CBV_{pa}/CBV_{pa}^{base}$), the relative difference became more apparent.

Figure 3 shows the calculated $CMRO_2$ changes during breath-hold and visual experiments using the Lu and Davis models. Note that as the Davis model employs BOLD, CBF, and CBV measurements during breath hold for calculating the calibration factor *M*, it can only estimate $CMRO_2$ dynamics in the visual task. Mean $\Delta CMRO_2/CMRO_2^{base}$ during the BOLD undershoot was calculated by averaging time points over the period marked by a dark horizontal bar. After breath-hold ends, $CMRO_2$ returned to baseline ($\Delta CMRO_2/CMRO_2^{base} = 0.9 \pm 7.7\%$). In contrast, $CMRO_2$ remained elevated ($P < 0.01$) for 20 to 25 seconds after termination of visual stimulation, which corresponds to the BOLD undershoot duration. The mean $\Delta CMRO_2/CMRO_2^{base}$ during BOLD undershoot estimated with Davis model ($15.4 \pm 7.8\%$) was higher ($P < 0.1$, notice large standard deviation) than the one estimated with Lu model ($10.6 \pm 7.4\%$). It is also intriguing to notice that the estimated $CMRO_2$ during breath hold slightly decreased from baseline ($P < 0.05$), which accords with some recent reports in animals (Zappe *et al*, 2008) and humans (Xu *et al*, 2011).

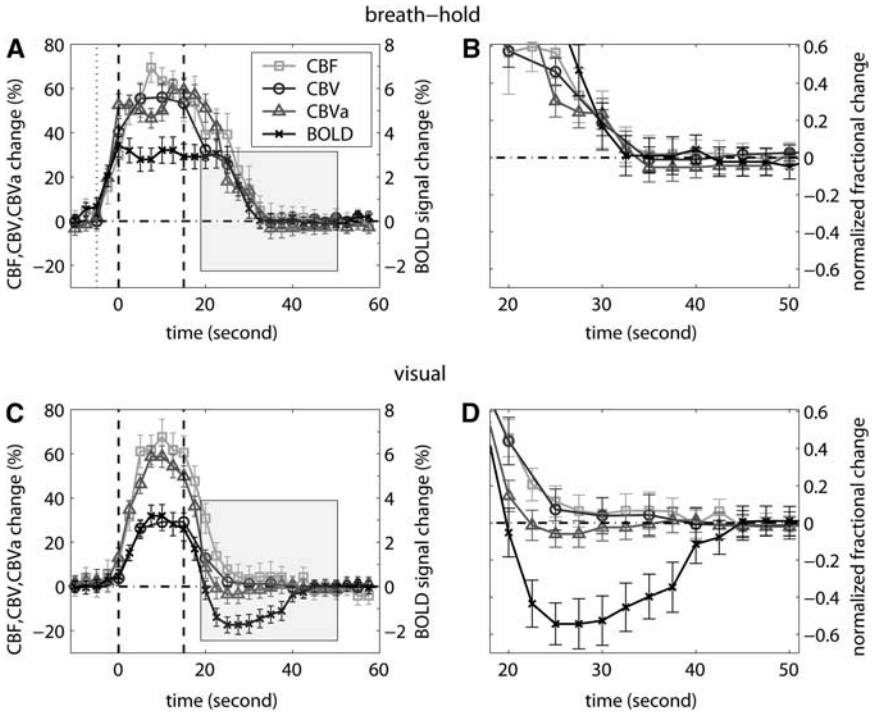

Figure 1 Average time courses of cerebral blood flow (CBF, square), cerebral blood volume (CBV; circle), arterial CBV (CBV_a; triangle), and blood oxygenation level-dependent (BOLD; cross) evolution during breath-hold (**A**, **B**) and visual (**C**, **D**) experiments. Time courses were first averaged over all blocks ($n = 4$) and subsequently over all subjects ($n = 10$). Error bars represent intersubject standard deviation. The relative signal changes ($\Delta S/S^{base}$) were displayed in **A** and **C**. For easier comparison, each time course was normalized by their individual maximum change and the shaded poststimulus periods in **A** and **C** were then zoomed in and displayed in **B** and **D**, respectively. The vertical dotted line in **A** denotes the beginning of exhaling before breath hold. The vertical dashed lines in **A** and **C** describe the start and end of the stimulus period. In **A** and **C**, the scale of CBF, CBV, and CBV_a change is labeled on the left and BOLD on the right. In **B** and **D**, the scale of the normalized signal (0 to 1) is labeled on the right.

Table 2 Mean time to reach baseline following cessation of breath hold and visual stimulation

	CBF (TILT)	*CBV (VASO)*	*CBV_a (iVASO)*	*BOLD*
Method I				
Breath –hold, seconds	20.7 ± 8.3	21.0 ± 8.7	18.3 ± 5.9	20.3 ± 8.6
Visual, seconds	13.9 ± 3.3	15.2 ± 6.3	7.2 ± 3.2	6.0 ± 6.2[a]
Method II				
Breath hold, seconds	20.5 ± 7.5	21.5 ± 9.7	17.9 ± 3.6s	21.0 ± 7.8
Visual, seconds	14.2 ± 4.1	15.1 ± 4.2	7.1 ± 3.9	6.4 ± 5.9[a]

BOLD, blood oxygenation level dependent; CBF, cerebral blood flow; CBV, cerebral blood volume; iVASO, inflow vascular space occupancy; TILT, transfer-insensitive-labeling technique.

[a]This is the first time for the BOLD time course to cross baseline after stimulus cessation. After the undershoot, the BOLD time course returned to baseline at 28.1 ± 5.5 seconds.

The mean time was calculated using the two approaches described in Materials and methods.

The standard deviation represents intersubject variation ($n = 10$, mean ± s.d.).

To evaluate the vascular and metabolic contributions to the undershoot, simulations were performed to predict BOLD signal changes from CBF, CBV, CBV_a, and $CMRO_2$ dynamics in the visual task, assuming that one of the two origins is absent. The amplitude of BOLD undershoot was defined as the absolute value of mean signal changes between 10 and 25 seconds (inclusive, four time points) after the visual stimulus was turned off. The results in Figure 4 show that the simulated total BOLD signal changes matched well with the measured BOLD time course (undershoot amplitude 1.26 ± 0.31%), verifying the accuracy of the calculation. When calculating the BOLD signal changes under the assumption that total CBV is at baseline ($\Delta CBV = 0$) during BOLD undershoot, the amplitude of the undershoot decreased to 0.89 ± 0.25% (Lu model) and 1.07 ± 0.33% (Davis model), respectively, 19.7 ± 15.9% and

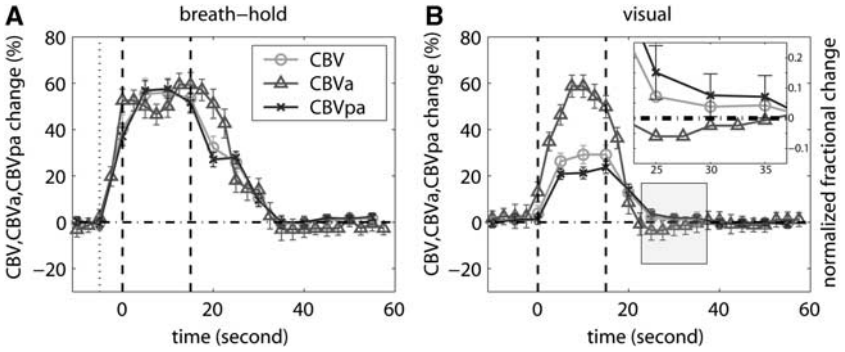

Figure 2 The average time courses of relative blood volume changes (percentage of baseline values) in arterial (arterial cerebral blood volume, CBV_a), postarterial (postarterial CBV, CBV_{pa}), and total (CBV) vascular compartments. The error bars represent intersubject standard deviation. For better visualization of small differences, the time courses in **B** were normalized by their individual peak height and the BOLD poststimulus undershoot period (shaded) was magnified in the inset. The vertical dotted line in **A** represents the beginning of exhaling before breath hold. The vertical dashed lines in both figures describe the start and end of the stimulation period.

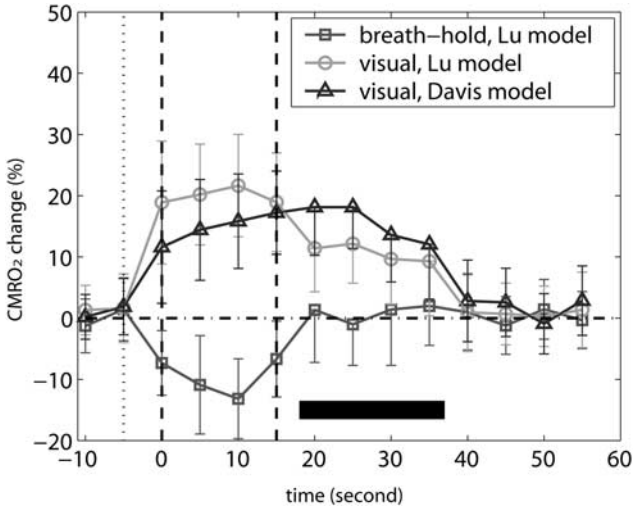

Figure 3 Estimation of cerebral metabolic rate of oxygen ($CMRO_2$) change using the Lu model for breath hold and Lu and Davis models for visual tasks. The $CMRO_2$ time courses were calculated for each subject and then averaged over all subjects ($n = 10$). The error bars represent intersubject standard deviation. For the time period corresponding to the BOLD poststimulus undershoot (20 to 40 seconds, marked by the dark horizontal bar), only the lower bounds of standard deviations are displayed, for the ease of comparing them with the baseline. The vertical dotted and dashed lines depict the beginning of exhaling before breath hold and the start and end of the stimulation period, respectively.

$12.7 \pm 22.5\%$ lower than the measured amplitude ($P < 0.1$). When performing simulations with the $CMRO_2$ change during undershoot artificially set to 0, the amplitude of the undershoot declined to $0.46 \pm 0.27\%$ (Lu) and $0.17 \pm 0.25\%$ (Davis), respectively, $78.7 \pm 18.6\%$ and $85.9 \pm 22.9\%$ smaller than the measured undershoot amplitude ($P < 0.01$).

It is important to analyze the potential error range of the estimated $CMRO_2$ changes from the adopted literature values for parameters in the Lu model. We repeated the data-processing procedure in Figures 3 and 4, while varying one of the parameters (Y_v^{base}, $R_{2a}^{*\,\text{base}}$, $R_{2v}^{*\,\text{base}}$, and $R_{2t}^{*\text{base}}$) by $\pm 20\%$ (Table 3). The calculated $\Delta CMRO_2/CMRO_2^{\text{base}}$ was the most sensitive to the baseline venous oxygenation fraction (Y_v^{base}), giving approximately 10% variation after visual stimulation. The baseline R^*_2 values of venous blood ($R_{2v}^{*\,\text{base}}$) and extravascular tissue ($R_{2t}^{*\text{base}}$) also affect the results slightly, whereas that of arterial blood ($R_{2a}^{*\,\text{base}}$) has negligible effects. Nevertheless, for all parameter values assumed ($\pm 20\%$), the calculated $CMRO_2$ changes were all at baseline ($P > 0.1$) and significantly elevated ($P < 0.01$) after breath hold and visual stimulation, respectively. The simulated BOLD signal changes assuming no $CMRO_2$ or CBV change during undershoot were all approximately 20% or 80% of the measured BOLD signal change, respectively.

Discussion

The disparity observed in BOLD signal behaviors after hypercapnic (no apparent undershoot) and visual (undershoot) stimulations allows investigation of the origins of BOLD undershoot. The first important observation is that, after visual stimulation, CBV_a returns to baseline before total CBV (Figure 1), whereas some residual vasodilation persists in the capillary and venous compartments (Figure 2). This residual CBV_{pa} dilation will contribute to the BOLD undershoot, similar to the delayed CBV recovery measured in many animal studies (Jones *et al*, 2001; Kida *et al*, 2007; Kim *et al*, 2007; Mandeville *et al*, 1998, 1999). The amplitude ($2.4 \pm 1.8\%$ of baseline CBV_{pa}) is in line with a recent study (Chen and Pike, 2009) that reported approximately 4% (of baseline CBV_{pa}) residual CBV_{pa} dilation during BOLD undershoot in human visual cortex at 3T. In contrast, after breath hold, both CBV_a and CBV_{pa} lingered above baseline for ~ 20 seconds.

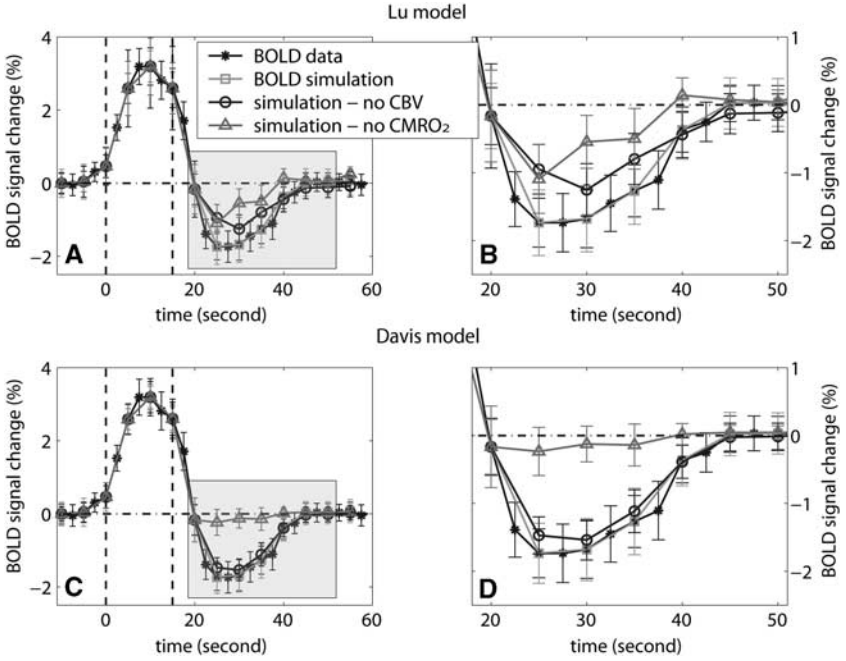

Figure 4 Estimation of the contributions from vascular compliance and sustained increased oxygen consumption to the blood oxygenation level-dependent (BOLD) poststimulus undershoot after visual stimulation obtained from simulating the BOLD signal change by assuming one origin to be absent. The measured BOLD data from the visual task and the BOLD signal changes simulated with original CBF/CBV/CBV_a measurements are plotted for reference. The Lu model (**A**, **B**) and Davis model (**C**, **D**) were employed to simulate BOLD signal changes under the assumptions that: (1) CBV returned to baseline 10 seconds after stimulation cessation (blue, circle) and (2) cerebral metabolic rate of oxygen staying at baseline 10 seconds after stimulus cessation (red, triangle). The time courses were averaged over all subjects ($n = 10$) and the error bars represent intersubject standard deviations. The shaded poststimulus periods in **A** and **C** were zoomed in and displayed in **B** and **D**, respectively. Note that the temporal resolution of the simulated time courses was limited by the lowest temporal resolution in our data, which is 5 seconds in the CBV measurement. The vertical dashed lines represent the start and end of the visual stimulation period.

Table 3 Error analysis for the baseline parameters used in the Lu Model

	$\Delta CMRO_2/CMRO_2^{base}$ *after breath hold*	$\Delta CMRO_2/CMRO_2^{base}$ *after visual*	*Contribution from CBV*	*Contribution from* $CMRO_2$
Original	0.9 ± 7.7%	10.6 ± 7.4%	19.7 ± 15.9%	78.7 ± 18.6%
Y_v^{base}				
−20%	1.4 ± 7.2%	9.8 ± 6.7%	22.4 ± 17.1%	75.6 ± 14.9%
+20%	−0.9 ± 7.6%	11.9 ± 7.8%	17.2 ± 14.9%	82.3 ± 15.6%
R_{2a}^{*base}				
−20	0.9 ± 7.8%	10.7 ± 7.4%	19.7 ± 15.3%	78.7 ± 18.2%
+20	0.7 ± 7.7%	10.5 ± 7.4%	19.6 ± 16.0%	78.7 ± 18.2%
R_{2v}^{*base}				
−20%	1.9 ± 7.4%	10.8 ± 7.9%	19.2 ± 16.1%	79.2 ± 18.9%
+20%	0.1 ± 6.7%	10.5 ± 8.4%	20.1 ± 15.9%	78.4 ± 17.9%
R_{2t}^{*base}				
−20%	0.4 ± 8.3%	10.5 ± 7.4%	19.8 ± 15.7%	78.5 ± 18.7%
+20%	1.3 ± 7.4%	10.7 ± 6.7%	19.4 ± 16.0%	78.9 ± 18.5%

BOLD, blood oxygenation level dependent; CBV, cerebral blood volume; $CMRO_2$, cerebral metabolic rate of oxygen.
To evaluate the potential errors arising from the baseline parameter values used in the Lu model, we reprocessed the data ($n = 10$) using a value 20% higher or lower than the literature values cited for baseline venous oxygenation fraction (Y_v^{base}), arterial (R_{2a}^{*base}), venous (R_{2v}^{*base}), and extravascular tissue (R_{2t}^{*base}) R^*_2s, respectively, while keeping the other parameters the same. The results were compared with the original ones reported in Materials and methods (Figures 3 and 4). The relative contribution from CBV/$CMRO_2$ change to the BOLD undershoot were estimated by comparing the simulated BOLD signal change when assuming the other source ($CMRO_2$/CBV change) is absent, with the measured BOLD signal change.

Note that the R^*_2 values of arterial and postarterial blood are smaller and larger, respectively, compared with that of extravascular tissue (at 3T, $R^*_2 = 21.15$ milliseconds for tissue (Lu and van Zijl, 2005), ≈ 16 milliseconds for arterial blood, and 31.3 to 47.2 milliseconds for postarterial blood (Zhao *et al*, 2007*b*)). Thus, elevated CBV_a and CBV_{pa} would have opposite effects on the overall BOLD signal, which may partly explain the absence of BOLD undershoot after breath hold. However, as the CBV_a^{base} fraction (≈ 0.2), residual CBV_{pa} dilation during undershoot, and difference between R^*_2s at 3T are all relatively small, the mismatch between CBV_a and CBV_{pa} dynamics alone is not adequate to fully explain the BOLD undershoot. Second, when looking at the $CMRO_2$ level after visual stimulation, it was clearly above baseline (10% to 15%) during the BOLD undershoot, as calculated by both the Lu model and Davis model (Figure 3). Conversely, $CMRO_2$ returned quickly to baseline after breath hold, where no BOLD undershoot was found. These results agree with previous studies (Donahue *et al*, 2009; Lu *et al*, 2004*b*) and reinforce the hypothesis that sustained increases in oxygen consumption have a large influence on the BOLD undershoot.

These data imply that the BOLD undershoot represents an aggregate consequence of both delayed capillary and venous (CBV_{pa}) blood volume recovery and persisting increases in oxygen metabolism. The relative contributions from vascular and metabolic origins were quantified with theoretical calculations (Figure 4), showing that delayed CBV_{pa} recovery and sustained increased oxygen metabolism contribute approximately $19.7 \pm 15.9\%$ and $78.7 \pm 18.6\%$, respectively. It should be noted that the relative size of these contributions can be temporally dependent. They were comparable at the beginning of undershoot when residual CBV_{pa} dilation was still sizable, whereas the elevated $CMRO_2$ dominated toward the end of undershoot. The contributions also have a spatial dependence as demonstrated by Yacoub *et al* and Zhao *et al* (Jin and Kim, 2008*a*; Yacoub *et al*, 2006; Zhao *et al*, 2007*a*) in their high-resolution ($0.15 \times 0.15 \times 2\,mm^3$) animal studies, which suggested that both vascular and metabolic mechanisms affect the BOLD undershoot in middle cortical layers, whereas increased oxygen metabolism in tissue is the reigning source in downstream pial vessels. In our human brain study at 3T, the spatial resolution was $3 \times 3 \times 3\,mm^3$ and, as such, our results may, in principle, have contributions from both parenchyma and surface vessels. However, by selecting cortical regions that were activated in all four imaging modalities, the majority of voxels containing large blood vessels were excluded.

One interesting observation found in our data is that the CBV_a time course in Figure 2 has a very slight dip after stimulus cessation. Although the mean CBV_a change is below baseline, the standard deviation is rather large so that it is not statistically significant. Table 2 shows that after visual stimulation, CBV_a returned to baseline ~ 5 seconds (limited by our temporal resolution) earlier than CBF. This is a little unexpected as CBF is mainly controlled by arterioles. Interestingly, a recent study (Devor *et al*, 2009) using two-photon microscopy showed, although in animal brains, a significant undershoot of arteriolar diameter after stimulus cessation, whereas the capillaries were still dilated for a few seconds before returning to baseline. We speculate that the small mismatch between arteriolar response and tissue perfusion could be because of neural activities that trigger arteriolar response slightly faster (Hillman *et al*, 2007) and then propagate through the rest of microvasculature. This phenomenon certainly deserves further validation and investigation, possibly by combining fMRI and high-resolution optics.

The accuracy of the quantitative results could be affected by the literature values used for the model parameters. In the Lu model, particularly, the baseline parameters (Y_v^{base}, $R_{2a}^{*\,base}$, $R_{2v}^{*\,base}$, and R_{2t}^{*base}) may vary between subjects. The blood R^*_2 values ($R_{2a}^{*\,base}$ and $R_{2v}^{*\,base}$) were measured in a circulating perfusion system with controlled oxygenation and temperature (Zhao *et al*, 2007*b*), which is probably still not totally reflective of the situation *in vivo*. This potential source of error was evaluated in Table 3 by giving each parameter a substantial deviation (20%) from the literature value and then recalculating the results. It shows that the estimated $\Delta CMRO_2/CMRO_2^{base}$ is the most sensitive to changes in Y_v^{base}, and moderately affected by $R_{2a}^{*\,base}$, $R_{2v}^{*\,base}$ and R_{2t}^{*base} changes. However, the potential error arising from these baseline parameters does not undermine the significance of the main conclusions in this study. For all parameters within a $\pm 20\%$ range, the $CMRO_2$ change was at baseline after breath hold while markedly increased after visual stimulation, and the relative contributions to the BOLD undershoot from residual CBV and $CMRO_2$ elevation were approximately 20% and 80%, respectively. Note that during the BOLD undershoot, the amplitudes of the BOLD/CBF/CBV/CBV_a changes are all much smaller (some at baseline) than those during stimulation. Therefore, the effects from the baseline parameter variations are expected to be magnified for the stimulation period, especially from Y_v^{base}. Fortunately, this parameter can be measured in a few minutes with some recently developed MRI techniques (Lu and Ge, 2008; Qin *et al*, 2011), which is recommended for future experiments to minimize the influence from the intersubject variation in Y_v^{base}.

The $CMRO_2$ change after visual stimulation and its relative contribution to the BOLD undershoot estimated by the Davis model are slightly greater ($P < 0.1$) than those from the Lu model. This discrepancy may be because of the fact that CBV_a and CBV_{pa} are treated as separate compartments in the Lu model, whereas in the Davis model, $\Delta CBV/CBV^{base}$ is used to

approximate $\Delta CBV_{pa}/CBV_{pa}^{base}$. Besides, the calibration factor M may alter between the breath-hold and visual sessions (Davis *et al*, 1998), which could introduce some error to the results. An intriguing result found in our data is that the estimated $CMRO_2$ using the Lu model slightly reduced during breath hold. Although this is somewhat controversial because it is generally believed that hypercapnia induces exclusively vascular response; a recent human study (Xu *et al*, 2011) has showed decreased brain activity during 5% CO_2 inhalation using MRI and electroencephalogram (EEG) techniques. In addition, recent animal studies have also shown suppressed neuronal activity during moderate hypercapnia (Zappe *et al*, 2008). These data suggest that the potential $CMRO_2$ change during hypercapnia may need to be accounted for when using the Davis model.

The major discrepancy between the vascular and metabolic hypotheses seems to be whether there is a substantial residual vasodilation during the BOLD undershoot. Functional studies in human brains using VASO (Donahue *et al*, 2009; Lu *et al*, 2004*b*; Poser and Norris, 2007; Tuunanen *et al*, 2006), contrast-agent-enhanced MRI (Blockley *et al*, 2009; Frahm *et al*, 2008), and optical spectroscopy (Schroeter *et al*, 2006) have reported that both CBV and CBF rapidly restore to baseline after stimulus termination, and that CBV values during BOLD undershoot are not significantly different from baseline. However, a number of studies in anesthetized animal brain have demonstrated that CBV responses measured with paramagnetic contrast-agent-enhanced MRI are slower than CBF response, and that approximately 5% to 10% remaining CBV dilation during BOLD undershoot is commonly observed (Kida *et al*, 2007; Kim *et al*, 2007; Mandeville *et al*, 1998, 1999). A few recent animal studies indicate faster CBV recovery after stimulus (Jin and Kim, 2008*a*, *b*). In this human study, we found that CBV_{pa} was slightly elevated ($P < 0.05$) during the BOLD undershoot, but the amplitude of this residual dilation (2% to 4%) was still smaller than in most animal studies. It is well known that the stimulus-induced signal change in paramagnetic contrast-agent-enhanced MRI is a collective result of the susceptibility effects from exogenous contrast agent and deoxygenated hemoglobin in blood, with the former reflecting CBV occupancy and latter known as the BOLD effect. It has been demonstrated that even at high iron dose (10 to 30 mg/kg), the BOLD effect still accounts for 10% to 30% of the observed signal change during stimulation at field strength ranging from 2 to 9.4 T (Lu *et al*, 2007; Mandeville *et al*, 1998), which may potentially confound the quantification of ΔCBV. During the undershoot, the BOLD effect reduces overall MR signal, thereby enhancing the negative signal change originating from superparamagnetic contrast agents. The amplitude of the BOLD undershoot can be as large as 30% to 60% of the peak positive BOLD signal change during stimulation (Frahm *et al*, 2008; Jin and Kim, 2008*a*). Therefore, we speculate that paramagnetic contrast-agent-enhanced MRI methods may slightly overestimate ΔCBV during undershoot, which may explain, in part, the apparent slow CBV return in many animal studies. This technical issue may deserve further investigation. Besides, as also pointed out by other researchers (Frahm *et al*, 2008; Jin and Kim, 2008*b*), factors such as the difference between human and animal brains, anesthesia techniques used in animal experiments, spatial resolution and partial volume averaging of tissue and blood vessels, voxel selection criteria, different cortical regions, and various stimulation types and durations may also contribute to this discrepancy.

Conclusions

To investigate the physiological sources of the BOLD poststimulus undershoot, multimodality fMRI experiments in human visual cortex at 3T were conducted to measure dynamic changes in BOLD, CBF, CBV, and CBV_a after breath hold and visual stimulation, respectively. During the temporal duration of the BOLD undershoot after visual stimulation, CBV_a quickly returned to baseline, whereas CBV_{pa} remained slightly elevated. The estimated $CMRO_2$ was at baseline after breath hold while remaining substantially elevated after visual stimulation. These results indicate that both delayed vascular compliance and continued oxygen metabolism may contribute to the poststimulus BOLD undershoot, with respective contributions estimated to be approximately 20% and 80%. Taken together, these data indicate the existence of transient physiological uncoupling between local oxidative metabolism ($CMRO_2$) and oxygen supply (CBF) during neural activities, a phenomenon that implies neurovascular coupling mechanisms such as the neurotransmitter pathway.

Acknowledgements

The authors thank Mr. Joseph S. Gillen, Ms. Terri Brawner, Ms. Kathleen Kahl, and Ms. Ivana Kusevic for experimental assistance.

Disclosure/conflict of interest

The National Center for Research Resources (NCRR) is a component of the National Institutes of Health (NIH). The contents of the paper are solely the responsibility of the authors and do not necessarily represent the official view of NCRR or NIH. Equipment used in the study is manufactured by Philips. Dr van Zijl is a paid lecturer for Philips Medical Systems. Dr van Zijl is the inventor of technology that is licensed to Philips. This arrangement has been approved by Johns Hopkins University in accordance with its conflict of interest policies.

References

Blockley NP, Francis ST, Gowland PA (2009) Perturbation of the BOLD response by a contrast agent and interpretation through a modified balloon model. *NeuroImage* 48:84

Buxton RB (2009) Modeling the effect of changes in arterial blood volume on the BOLD signal. In: *Proc 17th Annual Meeting ISMRM*. Hawaii, USA, 1620

Buxton RB, Wong EC, Frank LR (1998) Dynamics of blood flow and oxygenation changes during brain activation: the balloon model. *Magn Reson Med* 39:855

Chen JJ, Pike GB (2009) Origins of the BOLD post-stimulus undershoot. *NeuroImage* 46:559

Davis TL, Kwong KK, Weisskoff RM, Rosen BR (1998) Calibrated functional MRI: mapping the dynamics of oxidative metabolism. *Proc Natl Acad Sci USA* 95:1834–9

Dechent P, Schutze G, Helms G, Merboldt KD, Frahm J (2011) Basal cerebral blood volume during the post-stimulation undershoot in BOLD MRI of the human brain. *J Cereb Blood Flow Metab* 31:82–9

Devor A, Buxton RB, Tian P, Teng I, Lu K, L, Kurz R, Dale A (2009) From two-photon microscopy to BOLD-fMRI: association of an undershoot of arteriolar diameter with the BOLD post-stimulus undershoot. In: *Proc 17th Annual Meeting ISMRM*. Hawaii, USA, 509

Donahue MJ, Lu H, Jones CK, Edden RA, Pekar JJ, van Zijl PC (2006*a*) Theoretical and experimental investigation of the VASO contrast mechanism. *Magn Reson Med* 56:1261

Donahue MJ, Lu H, Jones CK, Pekar JJ, van Zijl PC (2006*b*) An account of the discrepancy between MRI and PET cerebral blood flow measures. A high-field MRI investigation. *NMR Biomed* 19:1043–54

Donahue MJ, Stevens RD, de Boorder M, Pekar JJ, Hendrikse J, van Zijl PC (2009) Hemodynamic changes after visual stimulation and breath holding provide evidence for an uncoupling of cerebral blood flow and volume from oxygen metabolism. *J Cereb Blood Flow Metab* 29:176

Frahm J, Baudewig J, Kallenberg K, Kastrup A, Merboldt KD, Dechent P (2008) The post-stimulation undershoot in BOLD fMRI of human brain is not caused by elevated cerebral blood volume. *NeuroImage* 40:473

Frahm J, Bruhn H, Merboldt KD, Hanicke W (1992) Dynamic MR imaging of human brain oxygenation during rest and photic stimulation. *J Magn Reson Imaging* 2:501

Frahm J, Kruger G, Merboldt KD, Kleinschmidt A (1996) Dynamic uncoupling and recoupling of perfusion and oxidative metabolism during focal brain activation in man. *Magn Reson Med* 35:143

Francis ST, Bowtell R, Gowland PA (2008) Modeling and optimization of Look-Locker spin labeling for measuring perfusion and transit time changes in activation studies taking into account arterial blood volume. *Magn Reson Med* 59:316

Golay X, Stuber M, Pruessmann KP, Meier D, Boesiger P (1999) Transfer insensitive labeling technique (TILT): application to multislice functional perfusion imaging. *J Magn Reson Imaging* 9:454–61

Hillman EM, Devor A, Bouchard MB, Dunn AK, Krauss GW, Skoch J, Bacskai BJ, Dale AM, Boas DA (2007) Depth-resolved optical imaging and microscopy of vascular compartment dynamics during somatosensory stimulation. *Neuroimage* 35:89

Hua J, Qin Q, Donahue MJ, Zhou J, Pekar J, van Zijl PCM (2009) Functional MRI using arteriolar cerebral blood volume changes. In: *Proc 17th Annual Meeting ISMRM*. Hawaii, USA, p. 12

Hua J, Qin Q, Donahue MJ, Zhou J, Pekar JJ, van Zijl PC (2011) Inflow-based vascular-space-occupancy (iVASO) MRI. *Magn Reson Med*; doi: 10.1002/mrm.22775

Jin T, Kim SG (2008*a*) Cortical layer-dependent dynamic blood oxygenation, cerebral blood flow and cerebral blood volume responses during visual stimulation. *Neuroimage* 43:1

Jin T, Kim SG (2008*b*) Improved cortical-layer specificity of vascular space occupancy fMRI with slab inversion relative to spin-echo BOLD at 9.4 T. *Neuroimage* 40:59

Jones M, Berwick J, Johnston D, Mayhew J (2001) Concurrent optical imaging spectroscopy and laser-Doppler flowmetry: the relationship between blood flow, oxygenation, and volume in rodent barrel cortex. *NeuroImage* 13:1002

Kida I, Rothman DL, Hyder F (2007) Dynamics of changes in blood flow, volume, and oxygenation: implications for dynamic functional magnetic resonance imaging calibration. *J Cereb Blood Flow Metab* 27:690–6

Kim T, Hendrich KS, Masamoto K, Kim SG (2007) Arterial versus total blood volume changes during neural activity-induced cerebral blood flow change: implication for BOLD fMRI. *J Cereb Blood Flow Metab* 27:1235

Kruger G, Kleinschmidt A, Frahm J (1996) Dynamic MRI sensitized to cerebral blood oxygenation and flow during sustained activation of human visual cortex. *Magn Reson Med* 35:797

Kwong KK, Belliveau JW, Chesler DA, Goldberg IE, Weisskoff RM, Poncelet BP, Kennedy DN, Hoppel BE, Cohen MS, Turner R (1992) Dynamic magnetic resonance imaging of human brain activity during primary sensory stimulation. *Proc Natl Acad Sci USA* 89:5675

Lin AL, Fox PT, Yang Y, Lu H, Tan LH, Gao JH (2008) Evaluation of MRI models in the measurement of CMRO2 and its relationship with CBF. *Magn Reson Med* 60:380–9

Lu H, Clingman C, Golay X, van Zijl PC (2004*a*) Determining the longitudinal relaxation time (T1) of blood at 3.0 Tesla. *Magn Reson Med* 52:679

Lu H, Donahue MJ, van Zijl PC (2006) Detrimental effects of BOLD signal in arterial spin labeling fMRI at high field strength. *Magn Reson Med* 56:546–52

Lu H, Ge Y (2008) Quantitative evaluation of oxygenation in venous vessels using T2-relaxation-under-spin-tagging MRI. *Magn Reson Med* 60:357–63

Lu H, Golay X, Pekar JJ, van Zijl PC (2003) Functional magnetic resonance imaging based on changes in vascular space occupancy. *Magn Reson Med* 50:263

Lu H, Golay X, Pekar JJ, Van Zijl PC (2004*b*) Sustained poststimulus elevation in cerebral oxygen utilization after vascular recovery. *J Cereb Blood Flow Metab* 24:764

Lu H, Law M, Johnson G, Ge Y, van Zijl PC, Helpern JA (2005) Novel approach to the measurement of absolute cerebral blood volume using vascular-space-occupancy magnetic resonance imaging. *Magn Reson Med* 54:1403

Lu H, Scholl CA, Zuo Y, Stein EA, Yang Y (2007) Quantifying the blood oxygenation level dependent effect in cerebral blood volume-weighted functional MRI at 9.4T. *Magn Reson Med* 58:616

Lu H, van Zijl PC (2005) Experimental measurement of extravascular parenchymal BOLD effects and tissue oxygen extraction fractions using multi-echo VASO fMRI at 1.5 and 3.0 T. *Magn Reson Med* 53:808

Mandeville JB, Marota JJ, Ayata C, Zaharchuk G, Moskowitz MA, Rosen BR, Weisskoff RM (1999) Evidence of a cerebrovascular postarteriole windkessel with delayed compliance. *J Cereb Blood Flow Metab* 19:679

Mandeville JB, Marota JJ, Kosofsky BE, Keltner JR, Weissleder R, Rosen BR, Weisskoff RM (1998) Dynamic functional imaging of relative cerebral blood volume during rat forepaw stimulation. *Magn Reson Med* 39:615

Nagaoka T, Zhao F, Wang P, Harel N, Kennan RP, Ogawa S, Kim SG (2006) Increases in oxygen consumption without cerebral blood volume change during visual stimulation under hypotension condition. *J Cereb Blood Flow Metab* 26:1043

Poser BA, Norris DG (2007) Measurement of activation-related changes in cerebral blood volume: VASO with single-shot HASTE acquisition. *Magma* 20:63

Poser BA, van Mierlo E, Norris DG (2011) Exploring the post-stimulus undershoot with spin-echo fMRI: implications for models of neurovascular response. *Hum Brain Mapp* 32:141–53

Qin Q, Grgac K, van Zijl PC (2011) Determination of whole-brain oxygen extraction fractions by fast measurement of blood T(2) in the jugular vein. *Magn Reson Med* 65:471–9

Schroeter ML, Kupka T, Mildner T, Uludag K, von Cramon DY (2006) Investigating the post-stimulus undershoot of the BOLD signal—a simultaneous fMRI and fNIRS study. *Neuroimage* 30:349–58

Tuunanen PI, Vidyasagar R, Kauppinen RA (2006) Effects of mild hypoxic hypoxia on poststimulus undershoot of blood-oxygenation-level-dependent fMRI signal in the human visual cortex. *Magn Reson Imaging* 24:993

van Zijl PC, Eleff SM, Ulatowski JA, Oja JM, Ulug AM, Traystman RJ, Kauppinen RA (1998) Quantitative assessment of blood flow, blood volume and blood oxygenation effects in functional magnetic resonance imaging. *Nat Med* 4:159

Woods RP, Grafton ST, Holmes CJ, Cherry SR, Mazziotta JC (1998) Automated image registration: I. General methods and intrasubject, intramodality validation. *J Comput Assist Tomo* 22:139

Woods RP, Mazziotta JC, Cherry SR (1993) MRI-PET registration with automated algorithm. *J Comput Assist Tomogr* 17:536

Xu F, Uh J, Brier MR, Hart J, Jr, Yezhuvath US, Gu H, Yang Y, Lu H (2011) The influence of carbon dioxide on brain activity and metabolism in conscious humans. *J Cereb Blood Flow Metab* 31:58–67

Yacoub E, Ugurbil K, Harel N (2006) The spatial dependence of the poststimulus undershoot asrevealed by high-resolution BOLD- and CBV-weighted fMRI. *J Cereb Blood Flow Metab* 26:634

Zappe AC, Uludag K, Oeltermann A, Ugurbil K, Logothetis NK (2008) The influence of moderate hypercapnia on neural activity in the anesthetized nonhuman primate. *Cereb Cortex* 18:2666–73

Zhao F, Jin T, Wang P, Kim SG (2007*a*) Improved spatial localization of post-stimulus BOLD undershoot relative to positive BOLD. *NeuroImage* 34:1084

Zhao JM, Clingman CS, Narvainen MJ, Kauppinen RA, van Zijl PC (2007*b*) Oxygenation and hematocrit dependence of transverse relaxation rates of blood at 3T. *Magn Reson Med* 58:592